

PAPER • OPEN ACCESS

Atmospheric extinction coefficients and night sky brightness at Bosscha Observatory

To cite this article: M Yusuf *et al* 2024 *J. Phys.: Conf. Ser.* **2773** 012003

View the [article online](#) for updates and enhancements.

You may also like

- [Bosscha Robotic Telescope \(BRT\) - a 0.35 meter telescope on Bosscha Observatory](#)
M. Yusuf, P. Mahasena, A.T. P. Jatmiko et al.
- [Light pollution at Bosscha Observatory, Indonesia](#)
Dhani Herdiwijaya
- [CCD observation of daylight crescent moon at Bosscha observatory](#)
P. Mahasena, M. Yusuf, M. Irfan et al.



ECS The Electrochemical Society
Advancing solid state & electrochemical science & technology

247th ECS Meeting
Montréal, Canada
May 18-22, 2025
Palais des Congrès de Montréal

Showcase your science!

Abstracts due December 6th

Atmospheric extinction coefficients and night sky brightness at Bosscha Observatory

M Yusuf¹, H I Arwinata^{1,2}, T Perhati¹, L Satya^{1,2}, A T P Jatmiko¹, D G Ramadhan¹, F Yap^{1,2}, S Ramadhan¹

¹ Bosscha Observatory, Faculty of Mathematics and Natural Sciences, Institut Teknologi Bandung, Indonesia

² Astronomy Study Program, Institut Teknologi Bandung, Indonesia

E-mail: m.yusuf@itb.ac.id

Abstract. We conducted a continuous sky brightness monitoring project in 2023 using the 14-inch (f/7.2) Bosscha Robotic Telescope (BRT) with Bessel filters at Bosscha Observatory. We present the initial measurement result of the extinction coefficient and sky brightness of three photometric nights from July to September 2023 using absolute photometry methods on photometric standard stars. The measurement results indicate the values of the first-order extinction coefficients span from $k'_b = 0.1344$ to 0.1596 , $k'_v = 0.0931$ to 0.1901 , $k'_r = 0.1208$ to 0.1592 , and $k'_i = 0.0836$ to 0.0967 with a typical error of 0.001 for two similar night. On September 12, our measurement results were $k'_b = 0.6186 \pm 0.0081$, $k'_v = 0.5404 \pm 0.0104$, $k'_r = 0.3684 \pm 0.0122$, $k'_i = 0.2483 \pm 0.0191$. Applying these values to the sky field reveals the average brightness in the V-band-pass, respectively 18.807 ± 0.061 , 18.999 ± 0.052 , and 18.867 ± 0.039 , with a color index $B - V$ of 0.421 ± 0.111 , 0.236 ± 0.094 and 0.426 ± 0.064 . The results are consistent with measurements from the transformed Sky Quality Meter (SQM) corresponding to the suitable filters.

1. Introduction

Sky brightness is the brightness value of the sky measured at the line-of-sight if no stars are present. Measuring the sky's brightness contribution accurately in star observation is crucial for precise stellar photometry [1]. In observations, sky brightness affects the signal-to-noise ratio (SNR) by increasing the amount of noise from the night sky. This means that SNR in bright skies is much lower compared to dark skies, and to obtain high-quality images and observation data, a higher SNR is required [2]. Hence, measuring sky brightness is of utmost importance in assessing the suitability of the location and timing for astronomical observations, such as deep sky imaging, photometry, and spectroscopy. Additionally, it substantially impacts the quality of observational data and the processing of photometric data.

2. Data

2.1. Instrument

Sky brightness measurements are performed at Bosscha Observatory ($107^{\circ}36'$ E, $6^{\circ}49'$ S, 1300 meters above sea level) using the Bosscha Robotic Telescope (BRT) [3] with a diameter of 14 inches and a focal ratio of f/7.2 with field of view (FoV) $48.38 \text{ arcmin} \times 32.26 \text{ arcmin}$. Equipped with a FLI Proline 11002 Monochrome charge-coupled device (CCD) with a gain of 0.73 and



readout noise of $17.1 e^{-1}$ at 12 MHz transfer data speed. In addition to the observations, we also used Unihedron's Sky Quality Meter (hereafter SQM) to confirm and compare the measurements at both detectors. This instrument consists of a photodiode with a visual filter effective in the wavelength range of 350-600 nanometers with a FoV 20° [4, 5].

2.2. Data Acquisition

Table 1. List of observed photometric standard stars.

No.	Star*	α (J2000.0)	δ (J2000.0)	$V \pm \sigma_V^{**}$	$B - V \pm \sigma_{(B-V)}$
1	HD 161304	17 44 51	00 08 05	8.525 ± 0.034	0.296 ± 0.054
2	BD-00 3353	17 45 20	00 25 52	9.331 ± 0.013	1.471 ± 0.028
3	IC 4665 54	17 45 29	05 49 21	11.601 ± 0.029	0.834 ± 0.062
4	HD 161480	17 45 34	05 42 56	7.680 ± 0.019	0.045 ± 0.031
5	IC 4665 52	17 45 39	05 36 24	12.097 ± 0.032	0.633 ± 0.078
6	HD 161542	17 45 55	05 54 28	7.494 ± 0.012	0.129 ± 0.024
7	IC 4665 60	17 46 00	05 36 40	11.319 ± 0.030	0.705 ± 0.056
8	HD 161573	17 46 07	05 31 49	6.841 ± 0.024	0.048 ± 0.039
9	CI* IC 4665 P 30	17 46 07	05 55 48	12.498 ± 0.035	0.727 ± 0.090
10	BD+05 3485	17 46 19	05 56 06	10.587 ± 0.016	0.431 ± 0.033
11	BD+05 3486	17 46 23	05 47 35	10.401 ± 0.024	0.320 ± 0.043
12	HD 161622	17 46 28	05 23 49	7.927 ± 0.025	0.452 ± 0.041
13	HD 161734	17 46 58	05 25 33	8.866 ± 0.023	0.130 ± 0.038
14	BD+05 3496	17 47 08	05 30 29	9.788 ± 0.024	0.689 ± 0.039
15	HD 162140	17 49 16	05 59 21	9.908 ± 0.013	0.473 ± 0.055
16	BD+05 3514	17 49 32	05 55 56	10.266 ± 0.061	1.077 ± 0.118
17	HD 162248	17 49 54	06 12 23	8.969 ± 0.078	1.314 ± 0.121
18	TYC 428-1951-1	17 50 02	06 05 57	11.936 ± 0.044	1.173 ± 0.070
19	[HH95] V380 Oph-4	17 50 20	06 03 44	12.301 ± 0.054	0.820 ± 0.077
20	TYC 568-1416-1	22 41 26	01 10 11	11.833 ± 0.001	0.656 ± 0.004
21	GSC 00568-01464	22 41 35	01 11 10	12.644 ± 0.004	0.965 ± 0.009
22	TYC 568-1298-1	22 41 37	00 59 06	11.599 ± 0.001	1.362 ± 0.002
23	SA 114-750	22 41 45	01 12 36	11.916 ± 0.001	-0.037 ± 0.001
24	BD+00 4910	22 42 08	01 16 49	10.909 ± 0.001	0.570 ± 0.001
25	TYC 568-1417-1	22 42 09	01 10 17	11.101 ± 0.003	1.206 ± 0.004

* Observed on July 18th, 2023 (no. 3-19), July 19th, 2023 (no. 1-19), and September 12th, 2023 (no. 20-25).

** Taken from Arne Henden CCD data (no. 1, 18 and 19), Sonoita Research Observatory or SRO data (no. 2), Bright Star Monitor–New Mexico or BSM–NM (no. 3–14), All Sky Automated Survey or ASAS (no. 15), The Amateur Sky Survey or TASS (no. 16–17), and Landolt 2009 (no. 20–25) [6].

We employ three types of images to measure sky brightness using absolute photometry (see section 3). First, we capture images of photometric standard stars with varying $B - V$ color indices to facilitate atmospheric and instrument extinction corrections. The list of these stars can be found in table 1. Second, we take an image of a sky region containing minimal bright stars with a sufficiently long exposure time to achieve a high SNR for measuring sky brightness near the zenith. Third, we acquire calibration images (bias, dark, and flat field) for data reduction. To conduct absolute photometry, we must ensure photometric sky conditions. Therefore, we

conduct observations over three available photometric nights at the Bosscha Observatory, with the zenith distance (Z) or air mass (X) coverage detailed in table 2.

Table 2. Observation dates and its air mass coverage.

Date	Time (UTC+7)	Z	X
July 18 th , 2023	20:22:12 – 04:33:55	5.303° – 70.723°	1.004 – 3.029
July 19 th , 2023	20:37:57 – 03:58:36	0.000° – 74.714°	1.000 – 3.793
September 12 th , 2023	21:46:47 – 04:37:27	5.052° – 36.268°	1.003 – 1.240

3. Method

3.1. Data Reduction and Aperture Photometry

We conducted image reduction using standard procedures to produce clean images, employing AstroImageJ (AIJ) version 5.2.1.04 [7]. Subsequently, aperture photometry [8] was performed on each standard star in the clean images using the **apphot** package within the Image Reduction and Analysis Facility (IRAF) version 2.17 [9]. Our aperture parameters included three times the Full Width at Half Maximum (FWHM) for the aperture size, 4.5 times the FWHM for the annulus, and one time the FWHM for the annulus width (dannulus) value. The result of this measurement provides the instrumental magnitude and its associated uncertainty.

3.2. Atmospheric Extinction and Instrument Correction

We use the absolute photometry method of the standard stars to measure the sky brightness. Standard stars' instrumental magnitude is converted to standard magnitude by atmospheric extinction and instrumental correction. Based on [10], the standard magnitude at λ -band-pass, M_λ , is generally defined in the following equation 1

$$M_\lambda = m_{\lambda 0} + \beta_\lambda C_S + \gamma_\lambda, \quad (1)$$

$$C_S = \delta C_0 + \gamma_{C_S}. \quad (2)$$

where $m_{\lambda 0}$ is the magnitude corrected for atmospheric extinction, β_λ is instrumental color coefficient, C_S is standard color index and γ_λ is instrumental zero-point constant. In C_S , δ is the color coefficient, C_0 is the color corrected for atmospheric extinction, and γ_{C_S} is the zero-point constant for the color.

3.2.1. First- and Second-Order Coefficient are determined to perform atmospheric extinction correction. From now on, we implement the method for magnitude v and color index $b - v$. The first-order coefficient k'_v is obtained for air mass correction. From equation 3, k'_v or k'_{bv} can be found by plotting v or $b - v$ versus X from star with small $b - v$ value

$$v = k'_v X + v_0. \quad (3)$$

We implement linear regression with the **curve_fit** module of the SciPy library [11] in Python. The slope of the line is k'_v .

To include the color dependence of the extinction coefficient, modify the first-order coefficient into $k'_v \rightarrow k'_v X + k'_v(b - v)$ and $k'_{bv} \rightarrow k'_{bv} X + k'_{bv}(b - v)$. Equation 3 become

$$v_0 = v - (k'_v + k''_v(b - v))X \quad (4)$$

$$(b - v)_0 = (b - v) - (k'_{bv} + k''_{bv}(b - v))X. \quad (5)$$

We used two stars with different color indices in the same air mass to solve equation 4 and 5, so that we get

$$\Delta v = k''_v \Delta(b - v)X + \Delta v_0 \quad (6)$$

$$\Delta(b - v) = k''_{bv} \Delta(b - v)X + \Delta(b - v)_0 \quad (7)$$

where Δ indicates the difference between the two stars. The solution of equation 6 and 7 is obtained from plotting Δv or $\Delta(b - v)$ versus $\Delta(b - v)X$ and the slope is the second-order extinction coefficient k''_v or k''_{bv} .

3.2.2. Zero-point Constant and Transformation Coefficient are determined to perform the instrumental correction. We have the following equation

$$V - v_0 = \epsilon(B - V) + \zeta_v \quad (8)$$

$$(B - V) - (b - v)_0 = (1 - 1/\mu_{bv})(B - V) + (\zeta_{bv}/\mu_{bv}) \quad (9)$$

where ϵ is the instrumental color coefficient, ζ_v is the instrumental zero-point constant, μ_{bv} is the color coefficient and ζ_{bv} is the zero-point constant for color. To solve equation 8 or 9, we used stars with different color indices in small air mass, less than 1.1. The solutions are obtained from plotting $V - v_0$ or $(B - V) - (b - v)_0$ versus $(B - V)$. The slope of the plot for equation 8 is ϵ and the intercept is ζ_v while for equation 9, the slope is $(1 - 1/\mu_{bv})$ and the intercept is ζ_{bv}/μ_{bv} .

3.3. Sky Brightness Measurement

We calculate the mean flux (intensity per seconds) in star-free areas of the sky images using AIJ. The mean flux is converted to the instrumental magnitude and multiplied by a constant to change its units to magnitude per arc second square (mpass). The instrumental magnitude in mpass can be substituted into equation 4 and 5, and the result v_0 and $(b - v)_0$ can be substituted to equation 8 and 9 to get the sky brightness in V and $B - V$ (in mpass unit).

4. Results and Discussion

By applying the method outlined in section 3, we compiled the extinction and transformation coefficient values for each night of observation in table 3. Illustrative plot examples for determining these coefficients and constants are shown in figure 1. The average difference between the star magnitude listed in table 1 and the calculated results, using the correction coefficient values obtained during the three nights of observation, is approximately 0.031 magnitude for both the V magnitude and the color index $B - V$ value.

The sky brightness at standard magnitude is determined by applying all the values listed in table 3. Meanwhile, the sky brightness obtained from the SQM needs to be converted into standard V magnitude by subtracting 0.56 magnitude from the SQM value, as stated by [4]. This adjustment is necessary because of the different sensor responses to the wavelengths in the Bessel V filter and the SQM.

The results of sky brightness measurements over three nights at the Bosscha Observatory are presented in table 4. Notably, the sky brightness values demonstrate consistent results when comparing the results of the absolute photometry method with the SQM measurements. Furthermore, we created a sky brightness map around the celestial equator, as depicted in figure 2, which illustrates that the sky brightness is darkest at the zenith and increases with zenith distance. Light pollution in the vicinity of the Bosscha Observatory could account for this pattern.

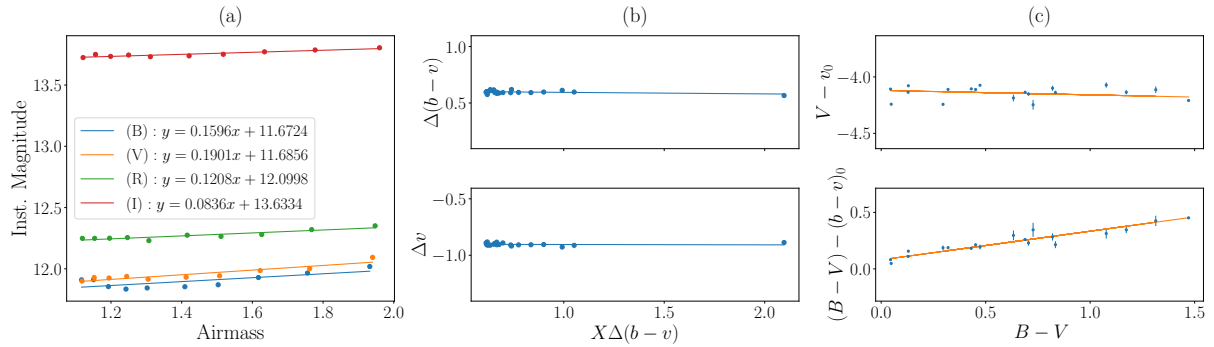


Figure 1. Correction coefficient and constant plot: (a) first-order extinction, (b) second-order extinction, and (c) transformation coefficient and zero-point value.

Table 3. Extinction coefficient, transformation coefficient, and zero-point constant.

Correction Coefficient & Constant	Date		
	July 18 th	July 19 th	September 12 th
k'_b	0.1344 ± 0.0011	0.1596 ± 0.0012	0.6186 ± 0.0081
k'_v	0.0931 ± 0.0009	0.1901 ± 0.0012	0.5404 ± 0.0104
k'_r	0.1592 ± 0.0008	0.1208 ± 0.0012	0.3684 ± 0.0122
k'_i	0.0967 ± 0.0008	0.0836 ± 0.0012	0.2483 ± 0.0191
k''_v	-0.0080 ± 0.0053	-0.0031 ± 0.0042	0.0015 ± 0.0141
k''_{bv}	-0.0175 ± 0.0066	-0.0135 ± 0.0051	-0.0402 ± 0.0258
ϵ	-0.0670 ± 0.0075	-0.0395 ± 0.0037	-0.0906 ± 0.0032
μ	1.2097 ± 0.0158	1.3398 ± 0.0097	1.2523 ± 0.0058
ζ_v	-4.2669 ± 0.0025	-4.1193 ± 0.0023	-3.6466 ± 0.0025
ζ_{bv}	0.2590 ± 0.0064	0.1074 ± 0.0056	0.3021 ± 0.0045

Table 4. Sky Brightness at Bosscha Observatory.

Sky Brightness (mpass)	Date		
	July 18 th	July 19 th	September 12 th
Absolute Photometry :	$Z = 5.74^\circ$	$Z = 8.65^\circ$	$Z = 10.73^\circ$
V_{sky}	18.807 ± 0.061	18.999 ± 0.052	18.867 ± 0.039
$(B-V)_{sky}$	0.421 ± 0.111	0.236 ± 0.094	0.426 ± 0.064
SQM :			
RAW	19.391 ± 0.032	19.752 ± 0.022	-
in V-band	18.831 ± 0.032	19.192 ± 0.022	-

Our values fall within the range of sky brightness values obtained by [12], which are 19.70 ± 0.84 and 19.01 ± 0.88 mpass. The relation between sky brightness and the month of observation also investigated by [12]. According to this data, our observations in July align with the measurements of [12]. On the other hand, our observations in September indicate that the

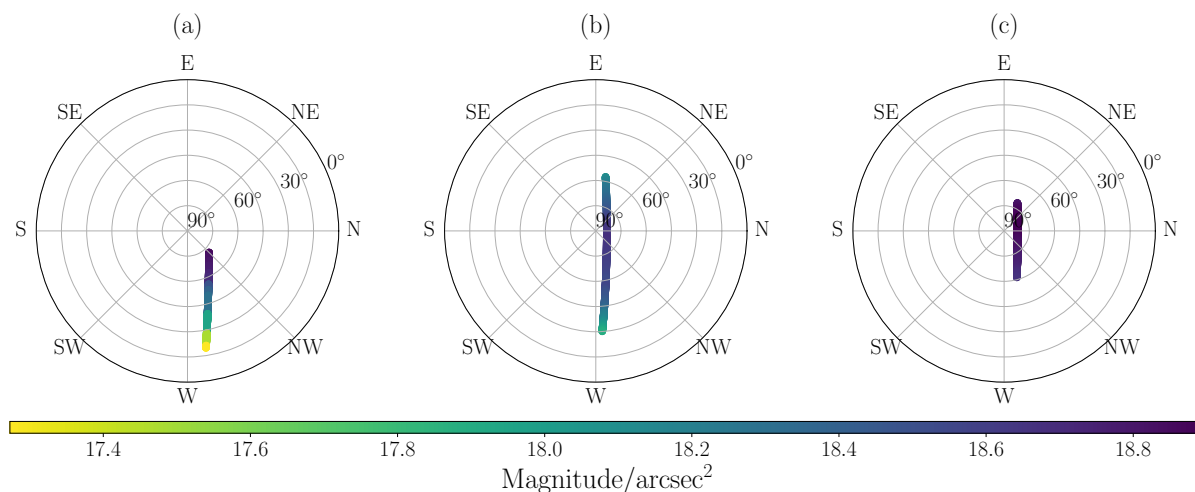


Figure 2. Sky brightness map at Bosscha Observatory: (a) July 18th, (b) July 19th and (c) September 12th, 2023.

sky brightness at Bosscha Observatory is darker than the measurements reported by [12].

5. Conclusions

We obtained the sky brightness values at Bosscha Observatory on July 18th and 19th, and September 12th, 2023, which are 18.807 ± 0.061 , 18.999 ± 0.052 , and 18.867 ± 0.039 based on absolute photometry method. Meanwhile, the sky brightness measured using SQM converted into standard V magnitude was obtained as 18.831 ± 0.032 and 19.192 ± 0.022 on July 18th and 19th, respectively. Our measurements show that the absolute photometry method and SQM measurement give consistent results. In addition, our results are also consistent with the measurements of [12]. In future work, we would like to map sky brightness over the entire sky area to determine the distribution of sky brightness at the Bosscha Observatory. Since our work is a long-term project, we will also map the sky brightness as a function of time to see its evolution.

References

- [1] Parker Joel W M 1999 *Publication of the Astronomical Society of the Pacific* **103** 243-52
- [2] Jacks A T 2021 (Indiana: Department of Physics/Astrophysics and Astronomy, Butler University)
- [3] Yusuf M, Mahasena P, Jatmiko A T P, Mandey D, Akbar E I, Setiawan A and Sulaeman M 2019 *J. Phys.: Conf. Series* **1127** 012045
- [4] Cinzano P 2005 *ISTIL Int. Rep* **9**
- [5] Fruck C *et al* 2015 *J. Inst.* **10** 04012.
- [6] Landolt A U 2009 *The Astronomical Journal* **137** 4186-269
- [7] Collins K A, Kielkopf J F, Stassun K G and Hessman F V 2017 *The Astronomical J.* **153** 77
- [8] Mighell K J 1999 *Precision CCD Photometry: ASP Conf. Series* **189** 50
- [9] Davis L E 1990 *A User's Guide to The IRAF Apphot Package*
- [10] Henden A A and Kaitchuck R H 1982 *Astronomical Photometry* (New York: Van Nostrand Reinhold) pp 25-30, 33-8 and 80-100
- [11] Virtanen P *et al* 2020 *Nature Methods* **17** 261-72
- [12] Herdiwijaya D, Satyaningsih R, Prastyo H A, Arumaningtyas E P, Sulaeman M, Setiawan A and Yulianty Y 2020 *Heliyon* **6** 8